DENTAL MATERIALS XXX (2021) XXX–XXX

Available online at www.sciencedirect.com

ScienceDirect

journal homepage: www.intl.elsevierhealth.com/journals/dema

Performance of crowns cemented on a fiber-reinforced composite framework 5-unit implant-supported prostheses: *in silico* and fatigue analyses

Edmara T.P. Bergamo[a], *Satoshi Yamaguchi*[b], *Adolfo C.O. Lopes*[a], *Paulo G. Coelho*[c,d,e], *Everardo N.S. de Araújo-Júnior*[a], *Ernesto B. Benalcázar Jalkh*[a,c,*], *Abbas Zahoui*[a], *Estevam A. Bonfante*[a]

[a] *Department of Prosthodontics and Periodontology, University of São Paulo - Bauru School of Dentistry, Bauru, SP, Brazil*

[b] *Department of Biomaterials Science, Osaka University Graduate School of Dentistry, 1-8 Yamadaoka, 565-0871, Suita, Osaka, Japan*

[c] *Department of Biomaterials, New York University College of Dentistry, New York, NY, USA*

[d] *Hansjörg Wyss Department of Plastic Surgery, NYU Langone Medical Center, New York, NY, USA*

[e] *Mechanical and Aerospace Engineering, NYU Tandon School of Engineering, Brooklyn, NY, USA*

ARTICLE INFO

Article history:
Received 10 March 2021
Received in revised form
2 September 2021
Accepted 13 September 2021
Available online xxx

Keywords:
Dental materials
Fiber-reinforced composite
Resin-matrix ceramics
Dental prosthesis
Dental implants

ABSTRACT

Objective. To characterize the biomechanical performance of fiber-reinforced composite 5-unit implant-supported fixed dental prostheses (FDPs) receiving individually milled crowns by *insilico* and fatigue analyses.

Methods. Eighteen implant-supported five-unit fiber-reinforced composite frameworks with an individually prepared abutment design were fabricated, and ninety resin-matrix ceramic crowns were milled to fit each abutment. FDPs were subjected to step-stress accelerated-life testing with load delivered at the center of the pontic and at 2nd molar and 1st premolar until failure. The reliability of the prostheses combining all loaded data and of each loaded tooth was estimated for a mission of 50,000 cycles at 300, 600 and 900 N. Weibull parameters were calculated and plotted. Fractographic and finite element analysis were performed.

Results. Fatigue analysis demonstrated high probability of survival at 300 N, with no significant differences when the set load was increased to 600 and 900 N. 1st and 2nd molar dataset showed high reliability at 300 N, which remained high for the higher load missions; whereas 1st premolar dataset showed a significant decrease when the reliability at 300 N was compared to higher load missions. The characteristic-strength of the combined dataset was 1252 N, with 1st molar dataset presenting higher values relative to 2nd molar and 1st premolar, both significantly different. Failure modes comprised chiefly cohesive fracture within the crown material originated from cracks at the occlusal area, matching the maximum principal strain location.

* *Corresponding author at*: Dept. of Prosthodontics and Periodontology, University of Sao Paulo – Bauru School of Dentistry, Al. Otávio Pinheiro Brisola 9-75, Bauru, SP, 17.012-901, Brazil.

E-mail address: ernestobenalcazarj@gmail.com (E.B. Benalcázar Jalkh).

https://doi.org/10.1016/j.dental.2021.09.008

Significance. Five-unit implant-supported FDP with crowns individually cemented in a fiber-reinforced composite framework presented a high survival probability. Crown fracture comprised the main failure mode.

1. Introduction

Implant-supported rehabilitations are a predictable treatment option to replace single or multiple teeth absences, greatly contributing to the recovery of the masticatory function and quality of life [1,2]. Porcelain fused to metal has been advocated in several studies as the standard of care for implant-supported reconstructions, especially for long-span prostheses [3,4]; however, esthetic concerns have motivated the indication of all-ceramic systems, i.e yttria-stabilized tetragonal zirconia polycrystals (Y-TZP) polycrystalline ceramics due to their favorable biocompatibility, biological and high mechanical properties (σ: 1200 MPa, K_{ic}: 9 MPa $m^{1/2}$, E: 210 GPa) [3–7]. Although high survival rates have been reported, approximately 95% after 5 years in function [3,4,7], implant-supported prostheses have exhibited higher levels of technical complications relative to tooth-supported prostheses, chiefly for Y-TZP reconstructions, which have not been limited to the metallic/Y-TZP framework fracture but mainly involved the integrity of the low-toughness veneering porcelain (K_{ic}: 0.7 MPa $m^{1/2}$ for Y-TZP and 1.1 MPa $m^{1/2}$ for metal ceramic) [8], with approximately 11–50% reported chipping after 5 years for fixed dental prostheses (FDPs) [3,7]. The rationale for the increased level of technical complications for implant-supported rehabilitations may lie on the absence of periodontal ligament and its inherent micromotion that helps to dampen occlusal forces, as well as mechanoreceptors and their feedback mechanism that differentiate food hardness and consistency [9–11]. Hence, technological improvements in the biomaterial science have been concentrated towards the development/improvement of biomechanically favorable restorative systems with occlusal forces dampening features to meet the functional and esthetic demands of dental reconstructions [9,10,12–17].

Fiber-reinforced composites (FRCs) have emerged as promising systems in several biomedical applications, particularly for their favorable strength- and stiffness-to-weight ratios [15–19]. Dental FRCs are generally composed of a high volume fraction of reinforcement compounds, carbon or glass fibers, bonded to a polymeric matrix by a coupling agent, where the fiber reinforcement bear the loads and increase the energy needed for crack propagation, known as resistance curve (R-curve) behavior, as well as increase the stiffness and strength of the material (σ: 540−740 MPa, K_{ic}: 9 MPa $m^{1/2}$, E: 30 GPa) [14,15,20]. Such properties of FRC composites are directly dependent on the fiber type and composition, fiber geometry and orientation, fiber volume fraction, polymer matrix, and quality of the fiber-matrix interface [14,21,22]. Given the typical anisotropic or orthotropic nature of conventional FRC reconstructions properties, the framework dimension and design as well as its three-dimensional position, usually following a structural relationship with occlusal forces distribution through a parallel alignment with the maximum principal stress direction, are key factors to obtain the maximum performance of FRC prostheses [14–17,19,22]. Moreover, FRC rehabilitations may offer significant clinical advantages due to their lower elastic modulus and increased resilience compared to metallic/Y-TZP rehabilitations, which may favor chewing forces absorption and stress distribution and improve the biomechanical performance of the restorations, particularly for implant-supported reconstructions [9,10,16,17]; as well as favorable cost effectiveness, chemical adhesion to resin composite and resin cement, and easy reparability with conventional in-office direct restorative procedures [14,15,18,21,23].

A systematic review has reported high survival rates, 94% after approximately 5 years in function for tooth-supported 3-unit FRC FDPs, similar to metallic/Y-TZP FDPs, with fracture of the veneering resin composite being the most reported technical complication, 9% [18]. Similarly, approximately 90% survival rate after 5 years have been calculated for implant-supported FRC FDPs, however the significant report of veneering resin composite fracture led to a considerably lower success rate, 70% after 5 years [24]. Such unfavorable events can be associated with an insufficient occlusal support provided by the unidirectional fiber alignment and hand-made processing of conventional FRC, which may increase defects population due to voids formation and compromise fiber-matrix interface, previously shown to affect the material strength up to 10% [14,15,18,25]; as well as, the challenging biomechanics inherent to implant-supported reconstructions [9–11]. Therefore, computer-aided design/computer-aided manufacturing (CAD/CAM) technologies have revolutionized FRC-based prostheses fabrication, potentially improving their clinical performance and range of indication [12,26]. FRC discs industrially fabricated under controlled conditions of temperature and pressure have shown to decrease defect population and to increase the material structural reliability, as well as to favor fibers interlacing and alignment in different directions [12,26–29]. While the milling process of CAD-CAM blocks have been primarily reported to be challenging, proper CAD designing and milling that consider fiber orientation can improve the biomechanical performance of the structure by enhancing framework/veneering material reliability, and therefore, reducing fractures [16,27,30–32]. Although the literature is still scarce in addressing FRC CAD/CAM systems clinical performance, fatigue testing, which has been considered a clinically relevant predictor of the mechanical behavior of dental rehabilitations [33,34], has demonstrated high probability of survival for implant-supported 3-unit FRC prostheses. The resin composite veneered onto FRC frameworks was the weak-

est link of the system, although the cohesive and adhesive observed fractures were not only repairable, but also occurred frequently above maximum bite forces [16].

New resin-matrix restorative systems for CAD/CAM use have been developed, named resin-matrix ceramics, where innovations in the polymerization mode, materials composition, ceramic particles reinforcement content, and microstructure have resulted in improved physicochemical and mechanical properties relative to conventional resin composites (σ: 190−270 MPa, E: 10−30 GPa [35–39]. Advantages of these materials also include a dense and reliable microstructure due to block/disc fabrication under an industrial environment, as mentioned for the FRC CAD/CAM processing, as well as excellent machinability and improved milling damage tolerance that may be linked to a small marginal gap, no need for firing, simple adjustment for optimal occlusion and polishing, and easy reparability [12,23,26,36,37]. Moreover, fatigue testing has shown high reliability for implant-supported single posterior reconstructions fabricated with resin-matrix ceramics [40]. Therefore, the combination of two polymeric systems modeled in an anatomical monolithic design and bonded following the CAD-on concept may further improve the biomechanical and esthetic behavior of polymeric reconstructions and broaden their range of indication to more functionally demanding clinical scenarios. In the present study, the mechanical behavior of an alternative rehabilitation concept, where an FRC framework was milled with an individual full-crown preparation design that allowed the cementation of crowns made of CAD/CAM resin matrix systems, in a challenging 5-unit posterior implant-supported fixed dental prosthesis (FDPs, from canine to second molar) using fatigue and *in silico* analyses was characterized. The rationale was to simulate a segment of a full-arch prostheses and the aims were: 1) to assess the probability of survival of the 5-unit FDP at 3 fatigued teeth (premolar and molars) individually and with all data combined; 2) to evaluate the failure modes by fractographic analysis and; 3) to observe the maximum principal strain location by finite element analysis (FEA).

2. Materials and methods

2.1. Sample preparation

Forty-two α-β titanium alloy (Ti-6Al-4V ELI) abutments for implants with a locking taper connection (Universal abutments, Bicon LLC, Boston, MA, USA) and 42 implants (3 mm well, 8 mm height, Bicon LLC) were acquired. Two implants per fixed dental prosthesis (FDP) were embedded using a surveyor (B2, Bio-Art, Sao Carlos, SP, Brazil) in polymethylmethacrylate acrylic resin (Classical, Campo Limpo Paulista, SP, Brazil) simulating 1 mm subcrestally implant placement and an inter-implant distance of 24 mm, which represented the dimensions to replace canine and second molar abutments and 1st and 2nd premolars and 1st molar as pontics. The respective abutments were tapped to the implants, the assembly was scanned and the model of a FDP including maxillary canine, 1st and 2nd premolars, and 1st and 2nd molars was virtually designed.

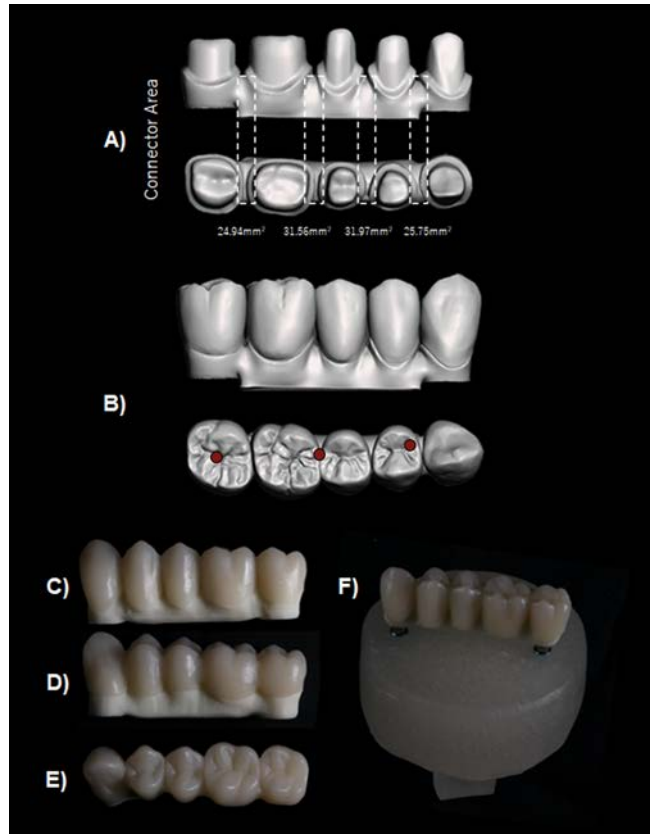

Fig. 1 – (A) Buccal and occlusal views of. stl file showing connector areas between prepared abutments: 24.9 mm² between molars, 31.5 mm² between first molar and second pre-molar, 31.9 mm² between premolars, and 25.7 mm² between canine and first premolar. (B) Final morphology of the. stl with crowns positioned showing on top a buccal and bottom a occlusal view. Red circles denote the areas designated for fatigue testing. (C), (D), and (E) are views of the milled 5-unit FRC framework with individual crowns cemented and the prostheses respective buccal, lingual, and occlusal views. (F) shows the implant-supported 5-unit FDP cemented on two abutments placed in 2 short implants embedded in polymethylmethacrylate for fatigue testing. (For interpretation of the references to colour in this figure legend, the reader is referred to the web version of this article.)

Through the created model, a fiber-reinforced composite (FRC, TRINIA, Bicon LLC, Boston, MA) infrastructure with an individual preparation design and connector areas presented in Fig. 1 was modeled and milled (n = 18). The FRC discs are comprised of 45 wt% epoxy resin matrix and 55 wt% multi-directional interlacing of glass fibers of approximately 10 μm diameter in several layers aligned in woven layers parallel to the top surface of the disc (E: 18.8 GPa/σ: 393 MPa, manufacturer data). The reported width and thickness of E-glass fibers are respectively 1.2–1.5 mm and 0.1–0.4 mm. [31] Also, single crown models were designed to restore the final form of the teeth and milled using a CAD/CAM resin matrix ceramic system (Shofu HC disc, Shofu, Kyoto, Japan). The resin matrix ceramic disc is composed of a methyl methacrylate resin

matrix and zirconium silicate ceramic particles (E: ~10 GPa/σ: 190 MPa, manufacturer data).

The FRC frameworks and crowns were finished and polished according to manufacturer's instructions. The FRC framework and the internal surface of the crown veneers were sandblasted with alumina particles of 45 μm for 10 s at a distance of 5 mm, washed, rinsed, and air dried. For adhesive bonding, a layer of primer followed by application of the bond system (CeraResin Bond, Shofu) was applied on the framework surface and intaglio surface of the crowns with a microbrush, and then light-cured for 20 s each surface (Valo Corded, Ultradent Products, South Jordan, UT, USA). The framework and the crowns were cemented using a dual-cure resin cement (BeautiCem SA, Shofu). For bonding, the resin cement was directly applied on the internal surface of the crowns using the cement automix dispenser. After setting, the assembly was maintained under a load of 10 N to allow uniform cement spreading and the excess was removed. The FDP margins were light-cured for 20 s on each surface. Subsequently, the FDP was cemented on the abutments using a dual-cure resin cement (BeautiCem SA, Shofu). The intaglio surface of the FRC abutments was previously sandblasted following the above-mentioned protocol. The samples were washed and rinsed and dried with compressed air. For bonding, the resin cement was directly applied on the internal surface of the FDP using the cement automix dispenser. After setting, the assembly was maintained under a load of 10 N to allow uniform cement spreading and the excess was removed. The FDP margins were light-cured for 20 s on each surface (Fig. 2). The samples were stored in deionized water for 48 h prior to mechanical testing [16,41].

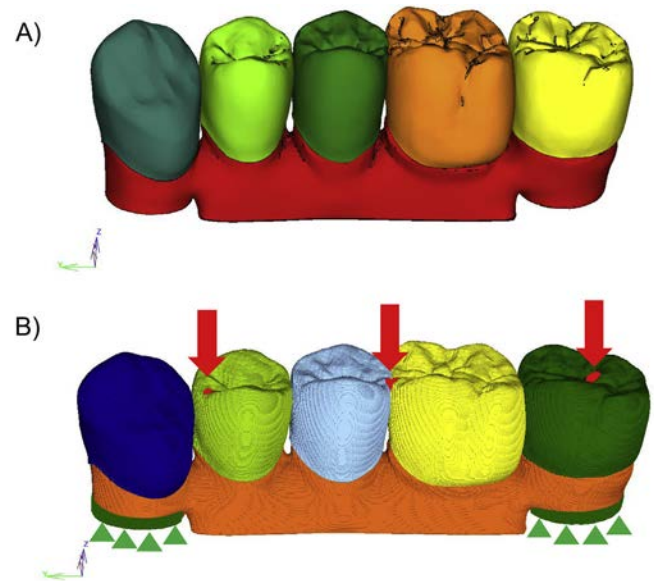

Fig. 2 – CAD model of the implant-supported 5-unit polymeric FDP used for finite element analysis (FEA) (A), where the stl. file was voxelized with 0.04 mm/voxel in the FEA software generating a number of voxels of 48,067,452 (B). Loading condition (300, 600, and 900 N) was based on the fatigue test data analysis, with same indentation areas on: (1) the mesial marginal ridge of the first premolar, (2) on the mesial marginal ridges of the second premolar and 1st molar; and (3) on the central fossa of the 2nd molar (Red arrows on B). (For interpretation of the references to colour in this figure legend, the reader is referred to the web version of this article.)

2.2. *Step-stress accelerated life testing (SSALT)*

Based on a previous fatigue test of FRC implant-supported prostheses [16], three stress profiles were used for SSALT: mild (n = 9), moderate (n = 6), and aggressive (n = 3), with the distribution of the specimens at a ratio of 3:2:1, respectively (n = 18/loaded area) [33]. These profiles are named based on the step-wise load increase that the specimen will be fatigued throughout the cycles until a certain level of load, meaning that specimens assigned to a mild profile will be cycled longer to reach the same load level of a specimen assigned to the aggressive profile. SSALT was performed using an all-electric dynamic test instrument (Electropuls E3000 Linear-Torsion system, Instron, Norwood, MA, USA) equipped with a 6.25 mm diameter spherical tungsten carbide indenter, with samples immersed in water at a frequency of 10 Hz. The load was sequentially applied in 3 regions of the same FDP: (1) first at the occlusal surface of the pontic on the mesial marginal ridge of the 1st molar and distal marginal ridge of the 2nd premolar. The test was conducted until specimen failure or suspension (absence of fracture until the end of the determined profile); (2) Fatigue testing continued on the same FDP at the central fossa of the 2nd molar using the same spherical indenter until specimen failure or suspension, and (3) at the mesial marginal ridge of the 1st premolar until specimen failure or suspension. Fatigue testing was continued only when failure was confined to the fatigued tooth, therefore not affecting the anatomy of the next area to be loaded and also that FRC framework did not fracture. The three loading regions (Fig. 1B and Fig. 2B) are expected to naturally occur in an Angle class I molar occlusion [42]. Fatigue loads throughout SSALT ranged from 200 N up to a maximum of 2000 N with a steady increase in load as a function of elapsed cycles and the findings were recorded as fracture load, stress profile and number of cycles in which the sample failed. Failure distribution were analyzed for all data combined (prosthesis survival), as well as for each individually loaded tooth.

Data analysis consisted of an underlying life distribution to describe the life data collected at different stress levels and a life-stress relationship to quantify the manner in which the life distribution changed across different stress levels [33,43,44]. Thus, the Weibull distribution was chosen to fit the life data collected in SSALT and its probability density functions (pdfs) would be given by: $\int(T) = \frac{\beta}{\eta}\left(\frac{T}{\eta}\right)^{\beta-1} e^{\left(\frac{T}{\eta}\right)^{\beta}}$, where η = scale parameter, and β = shape parameter. Considering the time-varying stress model ($x(t)$), the inverse power law relationship (IPL) was selected to extrapolate a use level condition considering the cumulative effect of the applied stresses, commonly referred as the cumulative damage model. In such a model, the IPL would be given by $L(x(t)) = (\alpha/x(t))^{\eta}$, where L = life data, and x(t) = stress. Then, the IPL-Weibull pdf (where η is replaced by the IPL) was given by: $\int(t, x(t)) =$

$\beta\left(\frac{x(t)}{\alpha}\right)^n\left(\int_0^t\left(\frac{x(t)}{\alpha}\right)^n du\right)^{\beta-1} e^{-\left(\left(\frac{x(t)}{\alpha}\right)^n du\right)^\beta}$. From the extrapolated use level pdf, a variety of functions was derived, including reliability $R(t, x(t)) = e^{-\left(\left(\frac{x(t)}{\alpha}\right)^n du\right)^\beta}$. Parameters estimation for all analyses was accomplished via maximum likelihood estimative (MLE) method, and 90% two-sided confidence interval (90%CI) was approximated using the Fisher matrix approach. Hence, the reliability was calculated for completion of a mission of 50,000 cycles at 300, 600, and 900 N and the differences between groups were identified based on the non-overlap of the CI (Synthesis 9, Alta Pro, Reliasoft, Tucson, AZ, USA). As the calculated use level probability Weibull beta parameter for some loaded areas were lower than 1, a Weibull 2-parameter calculation of the Weibull modulus, a unitless parameter that measures the variability of the results, and the characteristic strength, load at which 63.2% of the specimens would fail, was presented using the final load failure or survival (Weibull 9++, Reliasoft) [33,43,44]. Weibull 2-parameter contour plot (Weibull modulus vs. characteristic strength) was graphed to determine statistical differences through the non-overlap of CI.

2.3. *Fractographic analysis*

Failed FDPs were first inspected in polarized light stereomicroscope (AxioZoom V16, Zeiss, Oberkochen, Germany) using Z-stack mode which automates sequential imaging along the z-plane and sticks them within the same depth of focus (ZEN 2.3 PRO, Zeiss) to depict fracture planes and allow fractographic analysis under higher magnifications (up to 260x). Criteria used for failure were implant or abutment fracture, veneering crowns chipping (cohesive), veneering crowns fracture exposing the FRC framework (adhesive), and/or infrastructure fracture (catastrophic).

2.4. *Voxel based finite element analysis (FEA)*

The STL file was voxelized with 0.04 mm/voxel in the voxel-based FEA software (Voxelcon2015, Quint, Tokyo, Japan). Total voxel number was 48,067,452. Elastic modulus of the veneering material, resin composite block (Shofu Block HC, Shofu) was determined by following *in silico* non-linear dynamic three-point bending analysis, as established in previous work [45]. That of FRC composite was obtained from in-house data of manufacturer (Trinia, Bicon LLC). Poisson's ratio of each material was set to 0.38 according to that of dental composites [46] (Table 1). X, Y, and Z axes for FEA models were defined along bucco-lingual direction, mesio-distal direction, and axial direction, respectively. Static loads of 300 N, 600 N, and 900 N were loaded on three areas according to loading condition of *in vitro* fatigue testing. CAD/CAM resin composite crowns were perfectly cemented on the abutment and the bottom surface of the abutment was completely fixed along to X, Y, and Z axes. By following aforementioned boundary conditions, the voxel based FEA was conducted using matrix solver with an error of 0.0001 [47]. Maximum principal strain distribution was assessed, and maximum value was compared (Fig. 3).

3. Results

The cumulative damage model calculations using a Weibull distribution and an inverse power law life-stress relationship exhibited beta values (β, Weibull configuration factor) of 1.15 (confidence interval-CI: 0.76–1.76 when all data were collapsed and of 1.61 (CI: 0.55–4.75) for the 2nd molar, which indicate that fatigue damage accumulation was the main acceleration factor for failure. It is noteworthy that the lower bound of the CI of the fixed dental prostheses (FDPs) denotes an effect of strength influencing failure rate for such dataset ($\beta < 1$). On the other hand, beta values of 0.41 (CI: 0.09–1.81) for the 1st molar and of 0.25 (CI:0.09−0.65) for the 1st premolar indicate that materials strength was the main acceleration factor for failure. Again, it is worthy to mention that while the 1st premolar confidence bounds indicate a chief effect of strength influencing failure rate, the upper bound of the CI of the 1st molar indicate that fatigue damage accumulation also showed an effect on the failure rate.

Table 2 shows the probability of survival calculated for a mission of 50,000 cycles at 300, 600, and 900 N along with the bilateral 90% CI for the FDPs. Five-unit implant-supported prostheses with FRC frameworks demonstrated a high probability of survival (up to 94%, CI: 88–97 %) for an estimated masticatory molar load, 300 N. Moreover, no significant differences were observed when the set load was increased to 600 N (92%, CI: 84–96%) and 900 N (87%, CI: 74–94%), indicating high reliability for long-span FRC implant-supported prostheses. Similarly, data analyzed as a function of loaded area indicated high probability of survival for 1st and 2nd molars at 300 N (1st 100%, CI: 99–100%/2nd 98%, CI: 83–100%), as well as no significant differences were observed when the set load was increased to 600 N (1st 100%, CI: 98–100%/2nd 97%, CI: 71–100%), and 900 N (1st 99%, CI: 94–100%/2nd 94%, CI: 41–100%). Nonetheless, 1st premolar data analysis revealed high reliability at 300 N (83%, CI: 67–92%), whereas a progressive and statistically significant decrease in the probability of survival was observed at a set load of 600 N (23%, CI: 9–40%) and 900 N (0%). While 1st premolar data was only significantly lower than 1st molar at 300 N, they were significantly lower relative to all other set of data (all data, 1st molar, and 2nd molar) at 600 and 900 N.

The characteristic strength and the Weibull modulus of the 5-unit implant-supported prostheses are presented in the Fig. 4 and Table 3. Data analyzed as a function of fatigue load at failure using Weibull distribution depicted a Weibull modulus *(m)* of 2.17 (CI: 1.81–2.61) when all data of the prostheses were collapsed. The *m* values showed no significant difference for all loaded areas, 1st premolar (5.43, CI: 4.08–7.22) and 1st (5.94, CI: 4.29–8.24) and 2nd (5.56, CI: 4.04–7.64) molars, as observed by the overlap of the contours in the graph. The characteristic strength when all data of the FDP were collapsed was 1252 N (CI: 1123−1395 N). Concerning loaded area, the characteristic strength of the 1st molar (1779 N, CI: 1661−1906 N) was significantly higher than 2nd molar (1307 N, CI: 1215−1406 N)

Table 1 – Properties of the resin-matrix ceramic and fiber reinforced composite systems used for finite element analysis.

Product	Manufacturer	Elastic modulus (MPa)	Poisson's ratio
Veneering resin-matrix ceramic (Shofu HC)	Shofu	6,000	0.38
FRC Framework (TRINIA)	Bicon LLC	18,800	0.38
Abutment	Bicon LLC	114,000	0.34
Rely X U200	3M Oral Care	8,000	0.33

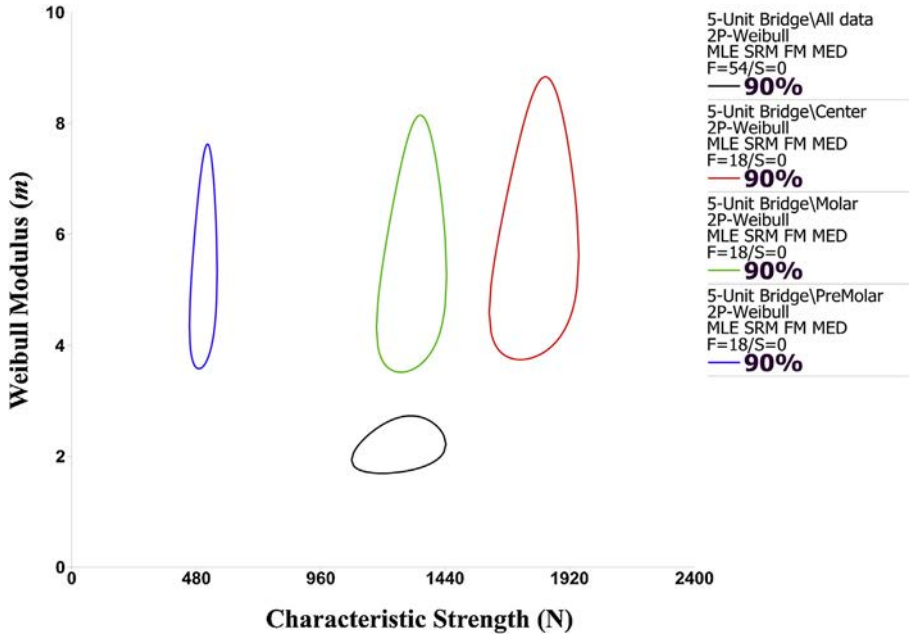

Fig. 3 – Contour plot evidencing the Weibull Modulus (*m*) and the Characteristic Strength (N) and of the implant-supported 5-unit polymeric FDP. The non-overlap of the contours indicates statistically significant difference.

Table 2 – Probability of survival (%) and the respective 90% confidence interval of the implant-supported 5-unit polymeric FDP for an estimated mission of 50,000 cycles at 300, 600, and 900 N.

	Lower bound	300 N	Upper bound	Lower bound	600 N	Upper bound	Lower bound	900 N	Upper bound
All data	88	94 aB	97	84	92 aB	96	74	87 aA	94
1st molar	99	100 aA	100	98	100 aA	100	94	99 aA	100
1st premolar	67	83 aB	92	9	23 bC	40	0	0 cB	0
2nd molar	83	98 aAB	100	71	97 aAB	100	41	94 aA	100

Different lowercase letters indicate statistically significant difference between missions. Different uppercase letters indicate statistically significant difference between FDP region.

Table 3 – Characteristic strength (N) and Weibull modulus of the implant-supported 5-unit polymeric FDP with the respective 90% confidence interval.

	Lower bound	Weibull modulus (*m*)	Upper bound	Lower bound	Characteristic strength (N)	Upper bound
All data	1.81	2.17 b	2.61	1123	1252 b	1395
1st molar	4.29	5.94 a	8.24	1661	1779 a	1906
1st premolar	4.08	5.43 a	7.22	469	506 c	546
2nd molar	4.04	5.56 a	7.64	1215	1307 b	1406

Different lowercase letters indicate statistically significant difference between FDP region.

and 1st premolar (506 N, CI: 469–546 N), both also statistically significant different.

The main failure modes demonstrated by the FDPs were the cohesive fracture of the resin-matrix ceramic crown at lower loads on the 1st premolar (chipping), as well as adhesive fracture of the veneering resin-matrix ceramic crown at higher loads on the 1st and 2nd molars (Fig. 5). Careful examination of the occlusal surface of the FDP revealed the typical wear of polymeric materials under the loading area before fracture. Cohesive fracture of the 1st premolar

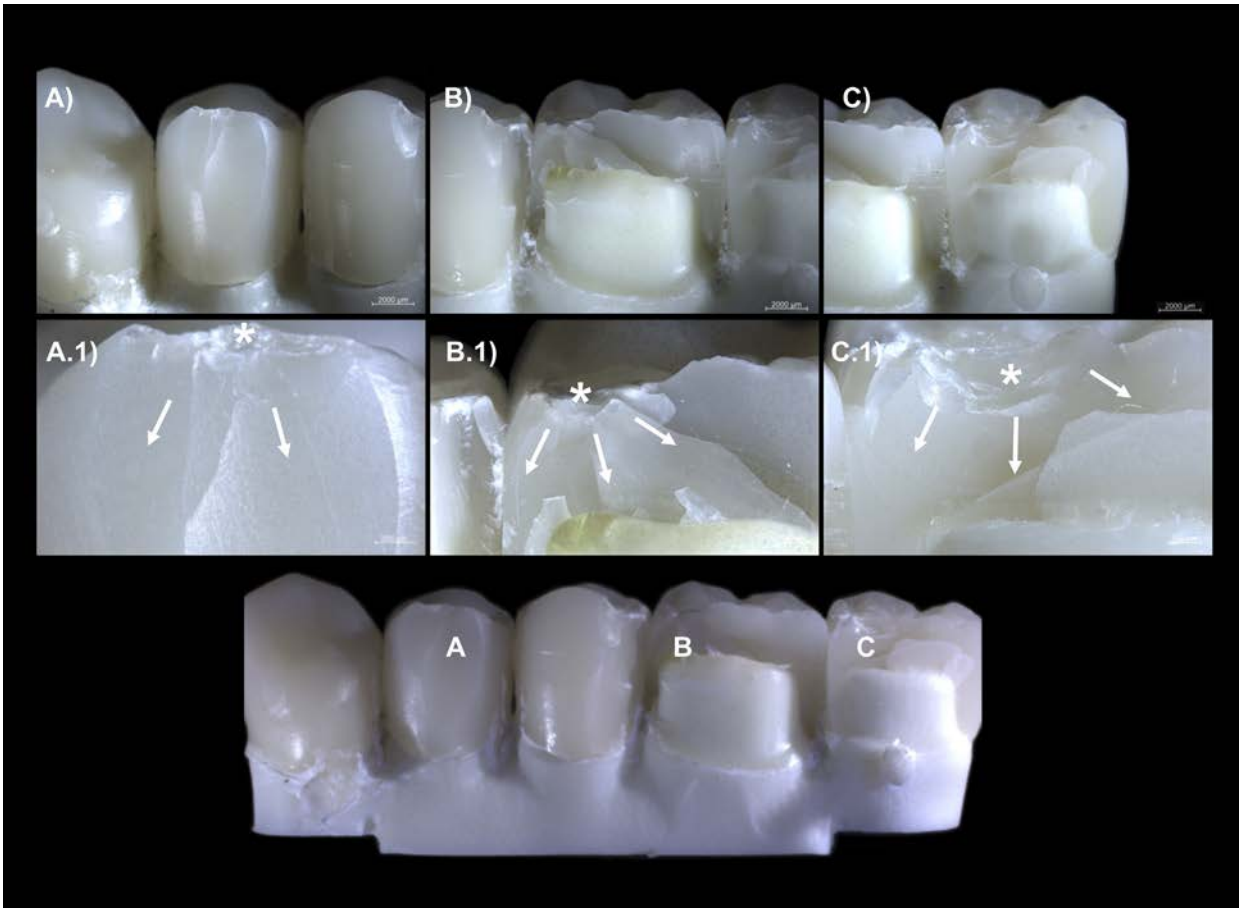

Fig. 4 – SEM images of a fractured implant-supported 5-unit FRC FDP (A). While 1st premolar (B) loading usually triggered cohesive fracture of the veneering crown, 1st (C) and 2nd (D) molar loading usually resulted in adhesive fracture of the veneering crown. The micrographs indicate the origin (*) and the direction of crack propagation (white arrows), with the crack initiating under the loading surface and propagating towards the proximal and cervical margins.

crown started from the occlusal indentation area, leading to subsurface damage and cone crack propagation towards the restoration cervical margins (Fig. 4A). Severe microcracking under the loading area was verified in the 1st and 2nd molars of the FDP with adhesive fracture, where cracks originating from multiple crack fronts propagated as the load and number of cycles increased and resulted in crown material delamination exposing the framework (Fig. 4B–C). Telltale fractographic marks including hackles and arrest lines confirmed the current findings. No framework fracture was observed. Neither implants nor abutments presented bending or fracture.

Maximum values of maximum principal strain after the voxel based FEA under 300 N, 600 N, and 900 N loadings were 0.252 $\mu\varepsilon$, 0.504 $\mu\varepsilon$, and 0.756 $\mu\varepsilon$, respectively. They were located at loading area in all loading conditions as shown in Figure 6.

4. Discussion

The restorative material has previously shown to influence the biomechanical performance of implant-supported reconstructions, especially for fixed dental prostheses (FDPs) [3,4,7,18,24]. The low elastic modulus inherent to the recently developed high-strength computer-aided design/computer-aided manufacturing (CAD/CAM) polymeric systems has become particularly relevant for implant-supported reconstructions by improving the capability to distribute occlusal forces and reduce stress transmission to the peri-implant bone since patients with implants have a decreased proprioception and lower tactile sensitivity [9–11]. Specifically, fiber-reinforced composites (FRC) advantages for framework milling may lie on their high strength-to-weight ratio, resistance-curve (R-curve) behavior, and reliability [15–21]. However, a proper CAD designing and milling, considering fiber orientation and providing FRC frameworks that favor fiber alignment are crucial [16,27,30–32]. Also, resin-matrix ceramics advantages for crown milling may lie on their improved strength relative to conventional resin composites, easy production and adjustment, high reliability and repairability [35–39]. Based on previous findings that have indicated the veneering resin composite as the weakest link of FRC reconstructions [16], the current study aimed to characterize the mechanical behavior of an alternative prosthesis

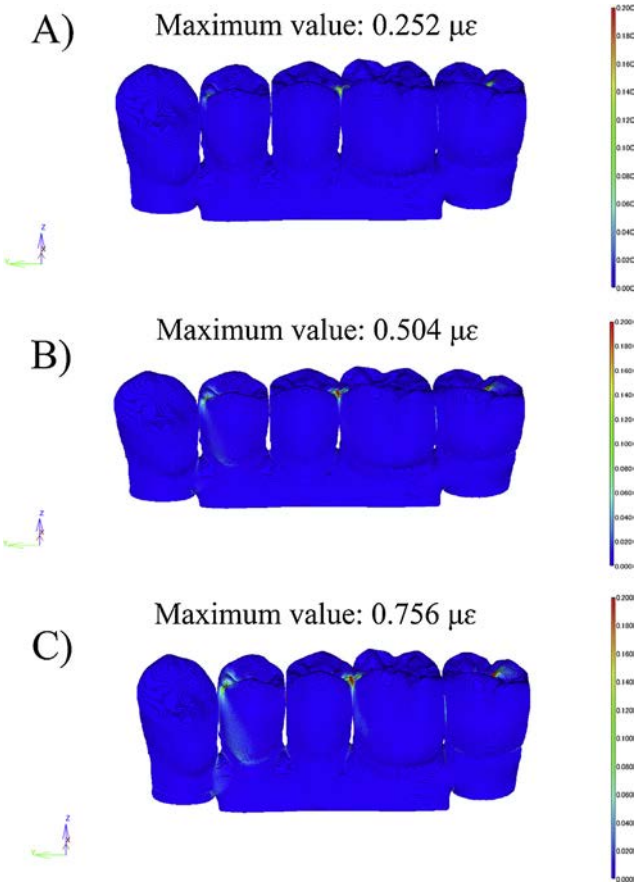

Fig. 5 – Maximum principal stress distribution on the implant-supported 5-unit FRC FDP under 300, 600, and 900 N.

design, where the milled FRC framework presented individual tooth preparations designed to allow for the cementation of resin-matrix ceramic crowns in a challenging 5-unit posterior implant-supported fixed dental prosthesis (FDPs) using step-stress accelerated-life fatigue testing (SSALT) and finite element analysis (FEA). Based on the obtained data, the FDPs presented high reliability for a masticatory molar load, 300 N, irrespective of loaded tooth. Moreover, in a more demanding loading scenario, 600−900 N, FDPs would maintain the estimated reliability at high levels, except for the 1st premolar data set. Despite at high loads, the main events for FDPs failure was cohesive and adhesive fracture of the veneering crown.

In FRC restorative systems, the polymer matrix binds the fibers transferring the load perpendicularly to fiber axis, and is supposed to guarantee mechanical, thermal, and chemical stability [14,15,19]. The FRC herein investigated basically consists of an epoxy resin matrix, which has previously demonstrated favorable moisture resistance, thermal conductivity, processing versatility along with satisfactory fracture toughness and strength, and low elastic modulus [48,49]. In addition, fiber content and their geometrical lay-up may influence the biomechanical performance of the rehabilitations [14–19,21]. The reinforcement compound of the FRC system consists of approximately 60% weight content of multi-directional glass fibers, which can be regularly interlaced due to the conformation of prefabricated discs under an industrial environment, minimizing the formation of defects and improving the flexural strength of the material up to 393 MPa, without increasing its elastic modulus (E: 30 GPa) [12,26–29]. Glass fibers have been widely used as reinforcing compounds in FRC systems due to their excellent thermal and chemical stability, as well as mechanical strength and wear resistance [50].

A resin-matrix ceramic system available in discs for milling was used as monolithic crowns individually cemented on the FRC framework. The physical-mechanical properties of resin-matrix ceramics are directly dependent on the size, distribution and weight content of the ceramic particles, as well as their incorporation into the polymer matrix that may influence the interfacial adhesion and presence of voids and defects, with systems composed of small particles and high filler content considered biomechanically advantageous [16,23,26,35–39]. The current system has previously shown to be composed of a methyl methacrylate polymer matrix and zirconium silicate ceramic nanoparticles and nanoclusters, where the dispersed ceramic compounds and the industrial blocks processing increased its flexural strength up to 190 MPa, approximately 100 MPa higher than conventional resin composites [26,37,36–39]. In fact, CAD/CAM processing in an industrial environment, inherent to both systems used in the current study, has shown to increase the structural reliability of restorative systems [12,26]. The Weibull modulus, a unitless parameter used to describe the variation in strength values and structural reliability as a result of flaw population [33,43,44,51], was approximately 5.0 for the different areas loaded in the FDP tested in the current study, which is within the range of values obtained for the currently available glass-ceramics and polycrystalline ceramic systems [35,40,41,51].

Failure rate interpretation based on the use level probability Weibull parameters for all data collapsed and only 2nd molar data set indicated that the fatigue accelerated failures ($\beta > 1$) through the cumulative damage triggered by the mechanical loading and environmentally assisted slow crack growth, commonly associated with late failures [23,33,34,41,44]. In contrast, the performance of the 1st premolar and 1st molar data set was mainly affected by materials strength rather than fatigue damage as cycles elapsed ($\beta < 1$) [16,23,40,41,44]. Nonetheless, confidence interval bounds indicated an influence of materials strength for the 2nd molar, as well as fatigue damage accumulation can also present a role on the 1st molar failure rate. Previous investigations on dental reconstructions using the SSALT methodology have shown similar failure rates [16,23,40,41,44].

SSALT data analysis have demonstrated high probability of survival (94%) for the long-span FDP at 300 N, physiologic masticatory molar load, with absence of significant differences when the set load was increased to 600 (92%) and 900 (87%) N, representing maximum voluntary bite forces [52]. Similarly, 1st and 2nd molars dataset showed high reliability at 300 N (∼98%), which remained high for the more demanding missions (∼97%); whereas 1st premolar data set showed a statistically significant decrease when the reliability at 300 N (83%) was compared to 600 (23%) and 900 (0%) N. Characteristic strength determined by the Weibull analysis considering the fatigue load-at-failure of the FDP was

1252 N, with 1st molar (1779 N) data set presenting significantly higher values relative to 2nd molar (1307 N) and 1st premolar (506 N), both significantly different. Despite 1st premolar inferior SSALT performance, the failure distribution was significantly higher than maximum bite forces in this area [52]. The promising biomechanical performance of the investigated FDPs design may be associated with the low elastic modulus and flexible nature of both polymer systems, FRC framework and resin-matrix ceramic crowns, making them more suitable for dampening occlusal forces and distributing stress [16,17]. Particularly, the resin-matrix ceramic used for machining the crowns has previously shown higher damage tolerance after fatigue testing relative to glass-ceramics, with approximately 60% less crack formation, which was associated with the more favorable elastic-plastic deformation and loading energy absorption capacity, which raise the critical load for crack initiation by reducing the stress intensity at critical defects (R-curve behavior) [53,54].

To the best of authors' knowledge, this is the first study using SSALT in a long-span CAD/CAM polymeric implant supported prosthesis scenario. Although an all-ceramic control group could be expected, it is important to acknowledge that porcelain fused to zirconia, which is the current all-ceramic alternative for implant-supported FDP (partial and full-arch) has shown unacceptable fracture rates of the porcelain veneer [7]. Data for monolithic zirconia use as long-span FDP is scarce and short-termed [55]. Previous studies using SSALT under a similar protocol for implant-supported 3-unit FRC FDPs with a conventional framework design of 12 mm^2 connector area and resin composite veneering have also demonstrated high reliability for a similar mission at 300 N (96%) [16]. Three-unit FDPs with 12 mm^2 connector area made of porcelain-fused to zirconia have resulted in a significantly lower survival than metal ceramic FDPs, which presented similar values to 3-unit FRC FDPs [41]. The comparison with the available data obtained for the standard of care indirect systems for long-span implant-supported prosthesis indicates a promising outcome for the newly proposed FRC framework design and monolithic single crowns veneering. Moreover, the results emphasize the principle that other properties besides mechanical strength may contribute to rehabilitations survival, especially in implant-supported reconstructions that seem to be more prone to technical complications due to the absence of periodontal ligament and its inherent impact absorption capacity [7,9,10,16,17,27].

Furthermore, the multidirectional alignment of the glass fibers along with the anatomic individual preparation design of the framework offered support to the resin-matrix ceramic single crowns, increasing load-at-fracture [14,16,17]. Continuous fibers parallelly aligned with the maximum principal stress direction has shown to get the maximum biomechanical performance of FRC rehabilitations [14–17,19]; however, clinical studies indicated that the most common failure mode of handmade conventional FRC prostheses with unidirectional fiber alignment is veneering material fracture at low loads as a result of framework insufficient occlusal support [14,18,24]; thus, the multidirectional fiber alignment along with the anatomic preparations to cement monolithic crowns, as herein investigated, potentially increased prosthesis fracture resistance and reduced fracture size, increasing repairability [16]. Despite the aforementioned improvements, the weakest link of FRC FDPs still comprised the veneering material by cohesive or adhesive fracture of the resin-matrix ceramic crowns, where cracks originated under the loading area propagated to the margins of the prostheses [16,35]. Voxel-based FEA has shown to be adaptable to complex CAD models such as FDPs and crowns and, consequently, used in this study to analyze crack initiation of the proposed CAD/CAM polymer reconstruction [56]. Maximum principal strain is a well-known failure criterion, effective to predict flexural strength of resin composites, and corroborated with the determined fracture origin in the fractographic analysis, under the loading area [57]. Moreover, an important advantage regarding such failure modes is the possibility of clinical repair, especially for cohesive failures of the 1st premolar area, through conventional in-office restorative procedures [15,16,58]. At higher loads (>1300 N), fractures were commonly larger, but still technically repairable. A previous study has demonstrated that the reliability of implant-supported resin-matrix ceramic crowns is maintained after in-office repairing when compared to its intact counterpart, suggesting more favorable results than resin composite repair in glass-ceramics and polycrystalline ceramics [23].

Concerning adhesive failures, the interfacial adhesion between the FRC, which consists of epoxy resin, and the resin-matrix ceramic crowns, composed of methacrylate-based resin, warrants further improvements since the solubility between both layers has shown to be compromised [59]. In fact, the adhesion between dental polymers through the formation of the well-known interpenetrating polymers network lies on the dissolution of the surface and polymer chain entanglement between the dissolved substrate of both framework and crown and monomers of resin cement; however, thermoset cross-linked polymers, such as the current FRC system, are difficult to dissolve without strong chemicals, high pressure or temperature, therefore affecting bond strength [60–62]. Another concern of the current indirect polymeric rehabilitation is the absence of the non-polymerized surface layer due to presence of air, which is common in direct polymer-based reconstructions, favoring a free radical polymerization and creating a more stable chemical bond [60]. Such aspects can be considered as limitations of the current FRC and resin-matrix ceramic systems and support further investigations concerning the use of different physicochemical surface pretreatments, including different protocols of sandblasting (i.e silica coating the alumina particles) and/or the development of different adhesive/primer systems, to improve surface dissolution of indirect polymeric systems and interfacial bond strength [14–17,19,59,63]. However, whether increased bond strength between resin composite and FRC framework, as well as increased mechanical properties of veneered material would synergistically translate to higher success rates are yet to be confirmed in clinical studies.

The current data suggest promising generations of high-strength polymeric systems that may provide a reliable treatment alternative, especially for implant-supported reconstructions where biomechanics is challenging, and

repair is commonly used to extend their lifetime. Further studies are required to determine their clinical performance.

5. Conclusion

Implant-supported fixed dental prostheses fabricated with fiber-reinforced composite frameworks with an individual preparation design that allowed cementation of resin-matrix ceramic single crowns resulted in a high probability of survival in a challenging posterior long-span prosthesis scenario. Crown fracture, cohesive and adhesive fracture, comprised the main failure mode. Such findings suggest a promising generation of polymeric systems for implant-supported reconstructions.

Acknowledgements

To Fundação de Amparo a Pesquisa do Estado de São Paulo (FAPESP) Young Investigators Award grant 2012/19078-7, EMU 2016/18818-8 and FAPESP scholarships 2019/08693-1, 2019/14798-0, 2018/03072-6/BEPE 2019/00452-5, to Conselho Nacional de Desenvolvimento Científico e Tecnológico (CNPq) grants 304589/2017-9 and 43487/2018-0, and to CAPES Finance Code 001.

REFERENCES

[1] Kumar Y, Chand P, Arora V, Singh SV, Mishra N, Alvi HA, et al. Comparison of rehabilitating missing mandibular first molars with implant- or tooth-supported prostheses using masticatory efficiency and patient satisfaction outcomes. J Prosthodont 2017;26:376–80.
[2] Chen ST, Buser D. Esthetic outcomes following immediate and early implant placement in the anterior maxilla—a systematic review. Int J Oral Maxillofac Implants 2014;29(Suppl):186–215.
[3] Sailer I, Strasding M, Valente NA, Zwahlen M, Liu S, Pjetursson BE. A systematic review of the survival and complication rates of zirconia-ceramic and metal-ceramic multiple-unit fixed dental prostheses. Clin Oral Implants Res 2018;29(Suppl 16):184–98.
[4] Pjetursson BE, Valente NA, Strasding M, Zwahlen M, Liu S, Sailer I. A systematic review of the survival and complication rates of zirconia-ceramic and metal-ceramic single crowns. Clin Oral Implants Res 2018;29(Suppl 16):199–214.
[5] Garvie RC, Hannink RH, Pascoe RT. Ceramic steel. Nature 1975;258:703–4.
[6] Guess PC, Schultheis S, Bonfante EA, Coelho PG, Ferencz JL, Silva NR. All-ceramic systems: laboratory and clinical performance. Dent Clin North Am 2011;55:333–52, ix.
[7] Pieralli S, Kohal RJ, Rabel K, von Stein-Lausnitz M, Vach K, Spies BC. Clinical outcomes of partial and full-arch all-ceramic implant-supported fixed dental prostheses. A systematic review and meta-analysis. Clin Oral Implants Res 2018;29(Suppl 18):224–36.
[8] Quinn JB, Quinn GD, Sundar V. Fracture toughness of veneering ceramics for fused to metal (PFM) and zirconia dental restorative materials. J Res Natl Inst Stand Technol 2010;115:343–52.
[9] Conserva E, Menini M, Tealdo T, Bevilacqua M, Ravera G, Pera F, et al. The use of a masticatory robot to analyze the shock absorption capacity of different restorative materials for prosthetic implants: a preliminary report. Int J Prosthodont 2009;22:53–5.
[10] Menini M, Conserva E, Tealdo T, Bevilacqua M, Pera F, Signori A, et al. Shock absorption capacity of restorative materials for dental implant prostheses: an in vitro study. Int J Prosthodont 2013;26:549–56.
[11] Meyer G, Fanghanel J, Proff P. Morphofunctional aspects of dental implants. Ann Anat 2012;194:190–4.
[12] Miyazaki T, Hotta Y, Kunii J, Kuriyama S, Tamaki Y. A review of dental CAD/CAM: current status and future perspectives from 20 years of experience. Dent Mater J 2009;28: 44–56.
[13] Silva NR, Witek L, Coelho PG, Thompson VP, Rekow ED, Smay J. Additive CAD/CAM process for dental prostheses. J Prosthodont 2011;20:93–6.
[14] Perea-Lowery L, Vallittu PK. Framework design and pontics of fiber-reinforced composite fixed dental prostheses — an overview. J Prosthodont Res 2018;62:281–6.
[15] Vallittu PK, Shinya A, Baraba A, Kerr I, Keulemans F, Kreulen C, et al. Fiber-reinforced composites in fixed prosthodontics—Quo vadis? Dent Mater 2017;33:877–9.
[16] Bonfante EA, Suzuki M, Carvalho RM, Hirata R, Lubelski W, Bonfante G, et al. Digitally produced fiber-reinforced composite substructures for three-unit implant-supported fixed dental prostheses. Int J Oral Maxillofac Implants 2015;30:321–9.
[17] Erkmen E, Meric G, Kurt A, Tunc Y, Eser A. Biomechanical comparison of implant retained fixed partial dentures with fiber reinforced composite versus conventional metal frameworks: a 3D FEA study. J Mech Behav Biomed Mater 2011;4:107–16.
[18] Ahmed KE, Li KY, Murray CA. Longevity of fiber-reinforced composite fixed partial dentures (FRC FPD)—systematic review. J Dent 2017;61:1–11.
[19] Gloria A, Ronca D, Russo T, D'Amora U, Chierchia M, De Santis R, et al. Technical features and criteria in designing fiber-reinforced composite materials: from the aerospace and aeronautical field to biomedical applications. J Appl Biomater Biomech 2011;9:151–63.
[20] Tiu J, Belli R, Lohbauer U. R-curve behavior of a short-fiber reinforced resin composite after water storage. J Mech Behav Biomed Mater 2020;104:103674.
[21] Freilich MA, Meiers JC. Fiber-reinforced composite prostheses. Dent Clin North Am 2004;48, viii–ix, 545–562.
[22] Vallittu PK. High-aspect ratio fillers: fiber-reinforced composites and their anisotropic properties. Dent Mater 2015;31:1–7.
[23] Bonfante EA, Suzuki M, Hirata R, Bonfante G, Fardin VP, Coelho PG. Resin composite repair for implant-supported crowns. J Biomed Mater Res B Appl Biomater 2016.
[24] Rossi F, Lang NP, Ricci E, Ferraioli L, Marchetti C, Botticelli D. 6-mm-long implants loaded with fiber-reinforced composite resin-bonded fixed prostheses (FRCRBFDPs). A 5-year prospective study. Clin Oral Implants Res 2017;28: 1478–83.
[25] Mehdikhani M, Gorbatikh L, Verpoest I, Lomov SV. Voids in fiber-reinforced polymer composites: a review on their formation, characteristics, and effects on mechanical performance. J Compos Mater 2019;53: 1579–669.
[26] Wendler M, Belli R, Petschelt A, Mevec D, Harrer W, Lube T, et al. Chairside CAD/CAM materials. Part 2: flexural strength testing. Dent Mater 2017;33:99–109.
[27] Rekow D, Thompson VP. Engineering long term clinical success of advanced ceramic prostheses. J Mater Sci Mater Med 2007;18:47–56.
[28] Muhlemann S, Benic GI, Fehmer V, Hammerle CHF, Sailer I. Clinical quality and efficiency of monolithic glass ceramic

crowns in the posterior area: digital compared with conventional workflows. Int J Comput Dent 2018;21:215–23.
[29] Sailer I, Benic GI, Fehmer V, Hammerle CHF, Muhlemann S. Randomized controlled within-subject evaluation of digital and conventional workflows for the fabrication of lithium disilicate single crowns. Part II: CAD-CAM versus conventional laboratory procedures. J Prosthet Dent 2017;118:43–8.
[30] Nagata K, Wakabayashi N, Takahashi H, Vallittu PK, Lassila LV. Fracture resistance of CAD/CAM-fabricated fiber-reinforced composite denture retainers. Int J Prosthodont 2013;26:381–3.
[31] Suzaki N, Yamaguchi S, Hirose N, Tanaka R, Takahashi Y, Imazato S, et al. Evaluation of physical properties of fiber-reinforced composite resin. Dent Mater 2020;36:987–96.
[32] Nagata K, Garoushi SK, Vallittu PK, Wakabayashi N, Takahashi H, Lassila LVJ. Fracture behavior of single-structure fiber-reinforced composite restorations. Acta Biomater Odontol Scand 2016;2:118–24.
[33] Bonfante EA, Coelho PG. A critical perspective on mechanical testing of implants and prostheses. Adv Dent Res 2016;28:18–27.
[34] Zhang Y, Sailer I, Lawn BR. Fatigue of dental ceramics. J Dent 2013;41:1135–47.
[35] Wendler M, Kaizer MR, Belli R, Lohbauer U, Zhang Y. Sliding contact wear and subsurface damage of CAD/CAM materials against zirconia. Dent Mater 2020;36:387–401.
[36] Lucsanszky IJR, Ruse ND. Fracture toughness, flexural strength, and flexural Modulus of new CAD/CAM resin composite blocks. J Prosthodont 2020;29: 34–41.
[37] Ruse ND, Sadoun MJ. Resin-composite blocks for dental CAD/CAM applications. J Dent Res 2014;93:1232–4.
[38] Mainjot AK, Dupont NM, Oudkerk JC, Dewael TY, Sadoun MJ. From artisanal to CAD-CAM blocks: state of the art of indirect composites. J Dent Res 2016;95:487–95.
[39] Horvath SD. Key parameters of hybrid materials for CAD/CAM-based restorative dentistry. Compend Contin Educ Dent 2016;37:638–43.
[40] Bonfante EA, Suzuki M, Lorenzoni FC, Sena LA, Hirata R, Bonfante G, et al. Probability of survival of implant-supported metal ceramic and CAD/CAM resin nanoceramic crowns. Dent Mater 2015;31:e168–77.
[41] Bonfante EA, Coelho PG, Navarro Jr JM, Pegoraro LF, Bonfante G, Thompson VP, et al. Reliability and failure modes of implant-supported Y-TZP and MCR three-unit bridges. Clin Implant Dent Relat Res 2010;12:235–43.
[42] Angle EH. Classification of malocclusion. Dent Cosmos 1899;41:350–75.
[43] Nelson W. Accelerated testing: statistical models, test plans and data analysis. John Wiley & Sons; 2004.
[44] Zhao WE, EA. A general accelerated life model for step-stress testing. IIE Trans 2005;37:1059–69.
[45] Karaer O, Yamaguchi S, Nakase Y, Lee C, Imazato S. In silico non-linear dynamic analysis reflecting in vitro physical properties of CAD/CAM resin composite blocks. J Mech Behav Biomed Mater 2020;104:103697.
[46] Greaves GN, Greer AL, Lakes RS, Rouxel T. Poisson's ratio and modern materials. Nat Mater 2011;10:823–37.
[47] Stocchero M, Jinno Y, Toia M, Jimbo R, Lee C, Yamaguchi S, et al. In silico multi-scale analysis of remodeling peri-implant cortical bone: a comparison of two types of bone structures following an undersized and non-undersized technique. J Mech Behav Biomed Mater 2020;103:103598.
[48] Patil R, Kankuppi S. Comparison between experimental and theoretical thermal conductivity on epoxy based aluminium hydroxide and silica aerogel composite materials. Mater Today Proc 2019;27:509–14.
[49] Atif R, Shyha I, Inam F. Mechanical, thermal, and electrical properties of graphene-epoxy nanocomposites—a review. Polymers 2016;8:1–30.
[50] Rajak DK, Pagar DD, Menezes PL, Linul E. Fiber-reinforced polymer composites: manufacturing, properties, and applications. Polymers 2019;11:1667.
[51] Tinschert J, Zwez D, Marx R, Anusavice KJ. Structural reliability of alumina-, feldspar-, leucite-, mica- and zirconia-based ceramics. J Dent 2000;28:529–35.
[52] van der Bilt A, Tekamp A, van der Glas H, Abbink J. Bite force and electromyograpy during maximum unilateral and bilateral clenching. Eur J Oral Sci 2008;116:217–22.
[53] Schlenz MA, Schmidt A, Rehmann P, Wostmann B. Fatigue damage of monolithic posterior computer aided designed/computer aided manufactured crowns. J Prosthodont Res 2019;63:368–73.
[54] Dogan DO, Gorler O, Mutaf B, Ozcan M, Eyuboglu GB, Ulgey M. Fracture resistance of molar crowns fabricated with monolithic all-ceramic CAD/CAM materials cemented on titanium abutments: an in vitro study. J Prosthodont 2017;26:309–14.
[55] Karasan D, Fehmer V, Ligoutsikou M, Srinivasan M, Sailer I. The influence of patient-related factors and material selection on the clinical outcomes of fixed and removable complete implant prostheses: an overview on systematic reviews. Int J Prosthodont 2021;34:s46–62.
[56] Yamaguchi S, Kani R, Kawakami K, Tsuji M, Inoue S, Lee C, et al. Fatigue behavior and crack initiation of CAD/CAM resin composite molar crowns. Dent Mater 2018;34:1578–84.
[57] Yamaguchi S, Mehdawi IM, Sakai T, Abe T, Inoue S, Imazato S. In vitro/in silico investigation of failure criteria to predict flexural strength of composite resins. Dent Mater J 2018;37:152–6.
[58] Rosentritt M, Behr M, Leibrock A, Handel G, Friedl KH. Intraoral repair of fiber-reinforced composite fixed partial dentures. J Prosthet Dent 1998;79:393–8.
[59] Alnaqbi IOM, Elbishari H, Elsubeihi ES. Effect of fiber post-resin matrix composition on bond strength of post-cement interface. Int J Dent 2018;2018:4751627.
[60] Vallittu PK. Interpenetrating polymer networks (IPNs) in dental polymers and composites. J Adhes Sci Technol 2009;23:961–72.
[61] Basavarajappa S, Perea-Lowery L, Alshehri AM, Al-Kheraif AAA, Matinlinna JP, Vallittu PK. Surface dissolution and transesterification of thermoset dimethacrylate polymer by dimethacrylate adhesive resin and organic catalyst-alcohol solution. Dent Mater 2020;36:698–709.
[62] Kallio TT, Lastumaki TM, Vallittu PK. Bonding of restorative and veneering composite resin to some polymeric composites. Dent Mater 2001;17:80–6.
[63] Xie Q, Lassila LV, Vallittu PK. Comparison of load-bearing capacity of direct resin-bonded fiber-reinforced composite FPDs with four framework designs. J Dent 2007;35:578–82.

Please cite this article in press as: Bergamo ETP, et al. Performance of crowns cemented on a fiber-reinforced composite framework 5-unit implant-supported prostheses: *in silico* and fatigue analyses. Dent Mater (2021), https://doi.org/10.1016/j.dental.2021.09.008